Localised $\mathrm{AdS}_5 \times \mathrm{S}^5$ Black Holes

Óscar J. C. Dias,[1,*] Jorge E. Santos,[2,†] and Benson Way[2,‡]

[1]STAG research centre and Mathematical Sciences, University of Southampton, UK
[2]Department of Applied Mathematics and Theoretical Physics,
University of Cambridge, Wilberforce Road, Cambridge CB3 0WA, UK

We numerically construct asymptotically global $\mathrm{AdS}_5 \times \mathrm{S}^5$ black holes that are localised on the S^5. These are solutions to type IIB supergravity with S^8 horizon topology that dominate the microcanonical ensemble at small energies. At higher energies, there is a first-order phase transition to AdS_5-Schwarzschild$\times\mathrm{S}^5$. By the Anti-de Sitter/Conformal Field Theory (AdS/CFT) correspondence, this transition is dual to spontaneously breaking the $SO(6)$ R-symmetry of $\mathcal{N}=4$ supersymmetric Yang-Mills down to $SO(5)$. We extrapolate the location of this phase transition and compute the expectation value of a scalar operator in the low energy phase.

Introduction – Since its discovery, the duality between type IIB supergravity on $\mathrm{AdS}_5 \times \mathrm{S}^5$ and $\mathcal{N}=4$ supersymmetric Yang-Mills (SYM) with large N gauge group $SU(N)$ and large t'Hooft coupling remains our best understood example of a gauge/gravity duality [1–4]. However, the properties of low-energy states[41] in these theories are mostly understood heuristically.

Consider black holes in type IIB supergravity on *global* $\mathrm{AdS}_5\times\mathrm{S}^5$, which are dual to gauge theory thermal states on a background spacetime conformal to $\mathbb{R}^{(t)} \times \mathrm{S}^3$. The duality requires the radius L of the S^5 to be the same as the length scale of the AdS_5. The most well-understood of such black holes are those that preserve the symmetries of the S^5, such as AdS_5-Schwarzschild$\times\mathrm{S}^5$ ($\mathrm{AdSSchw}_5 \times \mathrm{S}^5$). The horizon of these solutions is $\mathrm{S}^3 \times \mathrm{S}^5$. Since the S^5 is fixed, at low energies its entropy scales as $S \sim E^{3/2}$.

However, one expects the existence of spherical black holes that 'localise' on the S^5. These are black holes that are sufficiently small to appear point-like on the S^5 and are affected by the full 10-dimensional geometry. These have horizon topology S^8, so at low energies its entropy scales as $S \sim E^{8/7}$. They would therefore compete with $\mathrm{AdSSchw}_5 \times \mathrm{S}^5$ and dominate at low energies.

As the the size of these localised black holes is increased closer to the length scale L, one might expect this family to merge with 'lumpy' black holes [5]. These are topologically $\mathrm{S}^3 \times \mathrm{S}^5$ black holes that contain inhomogeneous deformations along the S^5 directions. The existence of lumpy black holes can be inferred from an instability of $\mathrm{AdSSchw}_5 \times \mathrm{S}^5$ black holes when their S^3 horizon radius is sufficiently small. Lumpy black holes branch off from $\mathrm{AdSSchw}_5 \times \mathrm{S}^5$ black holes at the onset of this instability [6]. (This instability and the existence of an inhomogeneous solution is analogous to the Gregory-Laflamme instability affecting black strings and other black objects with a separation of horizon length scales [7–13].)

Since localised black holes and lumpy black holes only exist for energy scales small compared to L, there must be a phase transition to $\mathrm{AdSSchw}_5 \times \mathrm{S}^5$ black holes. By the gauge/gravity duality, the symmetries of the S^5 are dual to the R-symmetry of $\mathcal{N}=4$ SYM. Black holes that do not respect the symmetries of the S^5 are therefore dual to thermal states with spontaneously broken R-symmetry where some scalar operators have developed a nonzero expectation value. In other words, this phase transition is between thermal states respecting the R-symmetry (dual to $\mathrm{AdSSchw}_5 \times \mathrm{S}^5$) at high energies, to thermal states with broken R-symmetry (dual to localised black holes) at low energies.

Beyond this qualitative picture, little is known about this phase transition. Though the onset of the instability was located in [6], later work [5] has demonstrated that lumpy black holes near this onset have less entropy than $\mathrm{AdSSchw}_5 \times \mathrm{S}^5$. Therefore, the onset of the instability cannot be the location of the phase transition and the transition must be first-order. Without further information about the localised black holes, the location of the phase transition, and the expectation value of the scalar operators in the broken phase remain unknown.

In this Letter, we construct these localised black holes numerically. We demonstrate that these solutions entropically dominate over $\mathrm{AdSSchw}_5 \times \mathrm{S}^5$ at small energies, extrapolate the location of the phase transition, and compute the expectation value of a scalar operator in the dual field theory. Through the duality, these results offer new quantitative predictions for $\mathcal{N}=4$ SYM.

Numerical Approach – The minimal field content in type IIB supergravity that can be asymptotically $\mathrm{AdS}_5 \times \mathrm{S}^5$ consists of a metric g and a self-dual 5-form $F_{(5)} = \mathrm{d}C_{(4)}$. Their equations of motion are

$$E_{MN} \equiv R_{MN} - \frac{1}{48} F_{MPQRS} F_N{}^{PQRS} = 0\,, \tag{1a}$$

$$\nabla_M F^{MPQRS} = 0\,, \tag{1b}$$

$$F_{(5)} = \star F_{(5)}\,. \tag{1c}$$

We seek static, topologically S^8 black hole solutions that are asymptotically $\mathrm{AdS}_5 \times \mathrm{S}^5$. Gravitational intuition suggests that the most symmetric of such black holes will have the largest entropy. These have $\mathbb{R}^{(t)}\times SO(4)\times SO(5)$ symmetry, where the full $SO(4)$ symmetry of AdS_5 and the largest subgroup of $SO(6)$ are preserved.

We use the DeTurck method [12–14], which requires the choice of a reference metric $\overline{g}$ that respects the same symmetries and causal structure as the desired solution. Consider the reference metric

$$\overline{\mathrm{d}s}^2 = \frac{L^2}{(1-y^2)^2}\bigg[-\frac{1}{L^2}H_1\mathrm{d}t^2 + \\ + H_2\left(\frac{4\,\mathrm{d}y^2}{2-y^2}+y^2\left(2-y^2\right)\mathrm{d}\Omega_3^2\right)\bigg] + \\ + L^2 H_2\bigg[\frac{16\,\mathrm{d}x^2}{2-x^2}+4x^2\left(2-x^2\right)\left(1-x^2\right)^2\mathrm{d}\Omega_4^2\bigg]\,, \tag{2}$$

where H_1, H_2 are functions which we will describe shortly. Note that if we set $H_1 = H_2 = 1$, this metric becomes global $\mathrm{AdS}_5\times\mathrm{S}^5$ [15]. Accordingly, we require that $H_1 = H_2 = 1$ at $y = 1$ to recover global $\mathrm{AdS}_5\times\mathrm{S}^5$ asymptotically. H_1 and H_2 must also be chosen so that the reference metric describes a regular S^8 black hole. It is also numerically desirable for the geometry near the horizon to approximate asymptotically flat Schwarzschild (Schw_{10}) when the black hole is small.

To help us choose H_1 and H_2 to satisfy these requirements, perform a change of coordinates

$$y = \sqrt{1-\mathrm{sech}\left(\rho\,\xi\sqrt{2-\xi^2}\right)}\,,$$
$$x = \sqrt{1-\sin\left(\frac{1}{2}\,\rho\left(1-\xi^2\right)\right)}. \tag{3}$$

This is essentially a Cartesian to polar map. To see this, the transformation $y = \sqrt{1-\mathrm{sech}(\mathrm{Y})}$ and $x = \sqrt{1-\sin(X/2)}$ maps the $\mathrm{d}x^2$ and $\mathrm{d}y^2$ components in the reference metric to $L^2H_2(\mathrm{d}X^2+\mathrm{d}Y^2)$, which is conformal to Cartesian coordinates. Finally, $X = \rho\xi\sqrt{2-\xi^2}$ and $Y = \rho(1-\xi^2)$ give the usual Cartesian to polar map with a different angular coordinate.

After the mapping, the reference metric (2) becomes

$$\overline{\mathrm{d}s}^2 = -M\frac{\left(\rho^7-\rho_0^7\right)^2}{\left(\rho^7+\rho_0^7\right)^2}\mathrm{d}t^2 + L^2H_2\bigg[\mathrm{d}\rho^2+\rho^2\bigg(\frac{4\mathrm{d}\xi^2}{2-\xi^2}+ \\ + G_1\xi^2(2-\xi^2)\mathrm{d}\Omega_3^2 + G_2\left(1-\xi^2\right)^2\mathrm{d}\Omega_4^2\bigg)\bigg], \tag{4}$$

where the map (3) uniquely determines G_1 and G_2, and relates M directly with H_1. In the $\mathrm{d}t^2$ component, the factor of $(\rho^7-\rho_0^7)^2/(\rho^7+\rho_0^7)^2$ is chosen in anticipation of placing a black hole horizon in the reference metric. Now set $H_2 = (1+\rho_0^7/\rho^7)^{4/7}$, which is consistent with our requirement that $H_2 = 1$ at $y = 1$ ($\rho\to\infty$). For small ρ and ρ_0, we have $G_1\approx G_2\approx 1$, so if $M\approx 1$, the reference metric would approximate Schw_{10} in isotropic coordinates. This guides our choice for H_1 (and consequently M and G_3). Choose H_1 so that $H_1 = 1$ at $y = 1$ ($\rho\to\infty$) and M is positive definite with $M = 1$ at $\rho = \rho_0$. The last requirement also fixes the temperature and ensures regularity of the horizon. Explicit expressions for H_1 and other known functions are given in the Supplementary Material.

With a reference metric, the DeTurck method modifies the Einstein equation (1a) to

$$E_{MN} - \nabla_{(M}\xi_{N)} = 0\,, \qquad \xi^M \equiv g^{PQ}[\Gamma^M_{PQ} - \overline{\Gamma}^M_{PQ}]\,, \tag{5}$$

where Γ^M_{PQ} and $\overline{\Gamma}^M_{PQ}$ define the Levi-Civita connections for g and $\bar{g}$, respectively. Unlike (1a), this equation yields PDEs that are elliptic in character. But after solving these PDEs, we must verify that $\xi^M = 0$ to confirm that (1a) is indeed solved. Local uniqueness properties of elliptic equations guarantee that solutions with $\xi^M = 0$ are distinguishable from those with $\xi^M \neq 0$. The condition $\xi^M = 0$ also fixes all coordinate freedom in the metric.

We choose a general ansatz that is consistent with the symmetries. The gauge potential takes the form

$$C_{(4)} = L^3F\,\mathrm{d}t\wedge\mathrm{dS}_{(3)} + L^4W\,\mathrm{dS}_{(4)}\,, \tag{6}$$

where F and W are unknown functions. The function W can be algebraically eliminated from the equations of motion and determined after the metric and F are known.

Our integration domain contains five boundaries: the horizon $\rho = \rho_0$, asymptotic infinity $y = 1$ ($\rho\to\infty$), the S_3 axis $y = 0$ ($\xi = 0$), the S^5 'north' pole $x = 1$ ($\xi = 1$), and the 'south' pole $x = 0$. For boundary conditions at infinity $y = 1$ ($\rho\to\infty$), we require global $\mathrm{AdS}_5\times\mathrm{S}^5$ asymptotics. The remaining boundary conditions are determined by regularity.

To handle the five boundaries numerically, we divide the integration domain into a number of non-overlapping warped rectangular regions or 'patches' as shown in Fig. 1. The four patches far from the horizon use $\{x, y\}$ coordinates, while the remaining patch uses $\{\rho, \xi\}$ coordinates. We require that the metric g, the form $C_{(4)}$, and their first derivatives match across patch boundaries.

We therefore have a boundary value problem for 7 functions in two dimensions. L drops out of the equations of motion, so the only parameter is ρ_0 which fixes the temperature [42]. We solve the system with Newton-Raphson using the reference metric and $f_7 = 1$ at $\rho_0 = 0.1$ as a first seed. We use pseudospectral collocation with transfinite interpolation of Chebyshev grids in each patch, and the linear systems are solved by LU decomposition. All solutions satisfy $\xi^2 < 10^{-10}$. More details, including explicit expressions for our ansatz and numerical convergence tests can be found in the Supplementary Material.

Results – In Fig. 2 we show the radii R_{Ω_3}, R_{Ω_4} of the geometrically preserved S^3 and S^4 along the horizon. This curve at small ρ_0 (high temperatures) is approximated by $R^2_{\Omega_3}+R^2_{\Omega_4}\approx 2^{4/7}\,\rho_0^2\,L^2$, implying that the horizon is nearly spherical. At larger ρ_0 (lower temperatures), the horizon is much more deformed.

Now we compute thermodynamic quantities. The temperature T is fixed by ρ_0. The entropy S is found by inte-

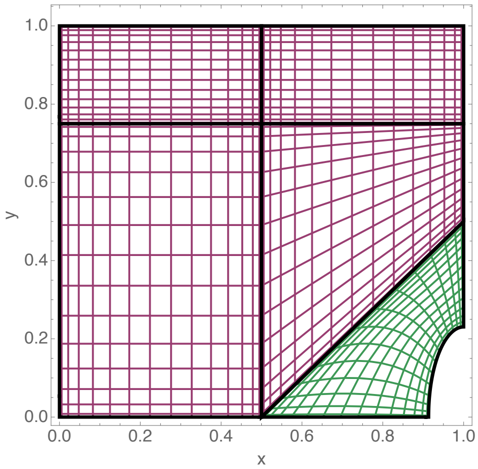

FIG. 1: Integration domain in $\{x, y\}$ coordinates. The green patch near the horizon is mapped from $\{\rho, \xi\}$ coordinates.

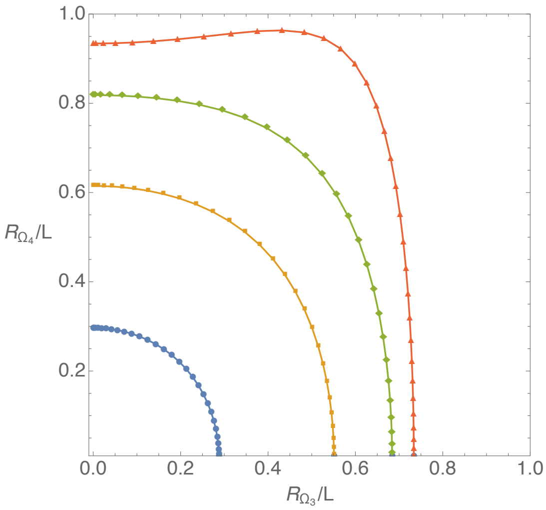

FIG. 2: Radii of the S^3 and S^4 along the horizon. From the bottom-left to the top-right $T = \{1.90, 0.945, 0.708, 0.538\}$.

grating the horizon area. The energy E is computed using the formalism of Kaluza-Klein holography and holographic renormalisation [5, 16–23] (see [5] and Supplementary Material for details). The AdS/CFT dictionary relates the 10 and 5 dimensional Newton constants to the number of colours N of $\mathcal{N} = 4$ SYM via $G_{10} = \frac{\pi^4}{2}\frac{L^8}{N^2}$ and $G_5 = \frac{G_{10}}{\pi^3 L^5}$. These thermodynamic quantities numerically satisfy the first law $\mathrm{d}E = T\mathrm{d}S$ to $< 0.1\%$ error.

In the microcanonical ensemble, the energy is fixed, and the dominant solution maximises the entropy. In Fig. 3, we show S/N^2 vs EL/N^2 for various competing solutions. The entropy is shown with respect to the entropy of AdSSchw$_5 \times \mathrm{S}^5$ [15, 24]. For small energies, the entropy of the localised black hole is well-approximated by that of Schw$_{10}$ and is larger than that of AdSSchw$_5 \times \mathrm{S}^5$.

For $EL/N^2 \lesssim 0.173$, AdSSchw$_5 \times \mathrm{S}^5$ black holes are unstable. We have found localised black holes for this energy range and determined that they have more entropy than AdSSchw$_5 \times \mathrm{S}^5$, indicating that localised black holes are a plausible endpoint to this instability.

At higher energies, the entropy of localised black holes approaches that of AdSSchw$_5 \times \mathrm{S}^5$, where we believe they will eventually meet in a first-order phase transition. Unfortunately, we were unable to reach this phase transition with our numerical resources. An extrapolation of data (see Supplementary Material for details) places the phase transition at $\{EL/N^2, S/N^2\} \approx \{0.225, 0.374\}$.

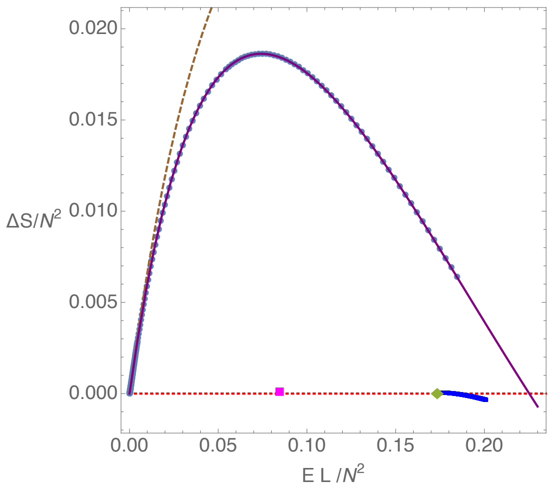

FIG. 3: Microcanonical phase diagram: entropy with respect to that of AdSSchw$_5 \times \mathrm{S}^5$ vs energy. The dotted red line is the AdSSchw$_5 \times \mathrm{S}^5$ phase, while the blue squares are the $\ell = 1$ lumpy black holes. The green diamond and magenta square mark the onset of the $\ell = 1$ and $\ell = 2$ Gregory-Laflamme instability, respectively. The solid purple curve and its points describe the localised black holes and a fit of its data. The brown dashed line is the lowest-order Schw$_{10}$ approximation.

As we have mentioned in the introduction, localised black holes are dual to a thermal state where the R-symmetry of $\mathcal{N} = 4$ SYM has been spontaneously broken (in our case down to $SO(5)$). This results in a condensation of an infinite tower of scalar operators with increasing conformal dimension. The lowest conformal dimension is 2, and the associated scalar operator is

$$\mathcal{O}_2 = \frac{2}{g_{\mathrm{YM}}^2}\sqrt{\frac{5}{3}}\,\mathrm{Tr}\left[(X^1)^2 - \frac{1}{5}\sum_{i=2}^{6}(X^i)^2\right], \qquad (7)$$

where X^i the are the six real scalars of $\mathcal{N} = 4$ SYM in the vector representation of $SO(6)$ and g_{YM} is the coupling constant (see e.g. [25] for the action of $\mathcal{N} = 4$ SYM). The expectation value $\langle\mathcal{O}_2\rangle$ in the broken phase can be found from the supergravity solution through the formalism of Kaluza-Klein holography [5, 16–23] (see also the Supplementary Material). We show $\langle\mathcal{O}_2\rangle$ for a range of energies in Fig. 4. Because the symmetry breaking transition is first-order, $\langle\mathcal{O}_2\rangle$ will have a nonzero value at the phase transition.

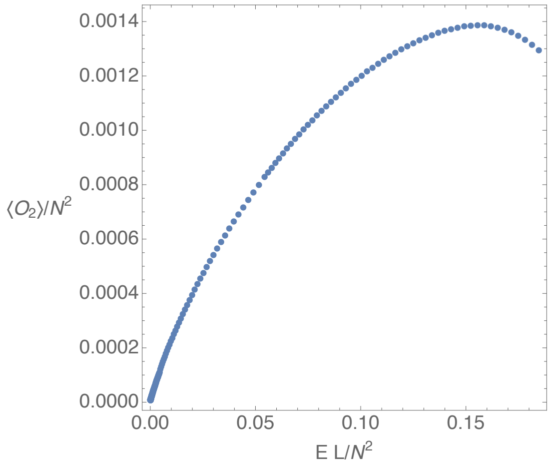

FIG. 4: Dimension 2 scalar condensate vs energy.

In the canonical ensemble, the temperature is fixed and the solution with lowest free energy $F = E - TS$ dominates. In this ensemble, there is the first-order Hawking-Page phase transition between large $\mathrm{AdSSchw}_5 \times \mathrm{S}^5$ black holes at higher temperatures and thermal $\mathrm{AdS}_5 \times \mathrm{S}^5$ at lower [15, 24]. All other known solutions, including localised black holes never dominate the canonical ensemble. (See the Supplementary Material for a phase diagram.)

Discussion – To summarise, we have numerically constructed asymptotically global $\mathrm{AdS}_5 \times \mathrm{S}^5$ localised black holes in type IIB supergravity. These black holes are topologically S^8 and are more entropic than any other known solution at low energies. At higher energies near $EL/N^2 \approx 0.255$, there is a first-order phase transition to $\mathrm{AdSSchw}_5 \times \mathrm{S}^5$ black holes. By the AdS/CFT correspondence, these localised black holes are dual to a thermal state of $\mathcal{N} = 4$ super Yang Mills (with large N gauge group and large t'Hooft coupling) with spontaneously broken R-symmetry. The scalar sector with the broken symmetry contains a dimension-2 operator with an expectation value shown in Fig. 4 and preserves a $SO(5)$ subgroup of the $SO(6)$ R-symmetry.

Since lattice simulations of field theories with holographic duals rely on finite temperature, numerical tests of AdS/CFT on both sides of the duality have been restricted to the canonical ensemble [26–32]. However, there has been recent progress in understanding first-order phase transitions in several ensembles [33–35]. We emphasise that such field theory calculations on $\mathcal{N} = 4$ SYM, at large t'Hooft coupling and large N, should reproduce both Fig. 3 and Fig. 4.

The completion of the phase diagram in Fig. 3 can be conjectured from other systems with Gregory-Laflamme instabilities [8–12, 36, 37] (see reviews [11, 13]). A family of lumpy black holes [5] (blue squares in Fig. 3) are connected to the onset of the Gregory-Laflamme instability (green diamond in Fig. 3). We expect the localised black holes to meet with the lumpy black holes in the space of solutions. For this to happen without violating the first law, there must be a cusp somewhere in the S/N^2 vs EL/N^2 curve. There must also be a topological transition point, which would be a solution with a naked singularity. Analogous systems with Gregory-Laflamme instabilities suggest that this topological transition point is closer to the lumpy black hole side of the curve. That is, that the cusp would be a topologically S^8 black hole.

Let us now comment on dynamical evolution. Entropy arguments suggest that the evolution of unstable $\mathrm{AdSSchw}_5 \times \mathrm{S}^5$ black holes would proceed towards the most dominant solution, which are the localised S^8 black holes. This entails a violation of cosmic censorship, much like in the evolution of the black string [38] or black ring [39]. Whether or not the evolution proceeds in this way, and the implications for $\mathcal{N} = 4$ SYM if cosmic censorship is violated remain important open problems. Interestingly, there is a range of energies $0.173 \lesssim EL/N^2 \lesssim 0.225$ where $\mathrm{AdSSchw}_5 \times \mathrm{S}^5$ is subdominant in entropy but nevertheless dynamically stable. In the field theory, this means that the time scale for spontaneous symmetry breaking at these energies is exponentially suppressed in N, compared to those at lower energies.

Many localised solutions dual to $\mathcal{N} = 4$ SYM states remain to be studied. In global $\mathrm{AdS}_5 \times \mathrm{S}^5$, there are localised solutions that break more symmetries, but these are likely less entropic than the ones preserving $SO(5)$. There are other localised solutions arising from higher harmonics of the Gregory-Laflamme instability. In particular, the $\ell = 2$ mode (whose onset is shown in Fig. 3) leads to double S^8 black holes and $\mathrm{S}^4 \times \mathrm{S}^4$ 'black belts' [5]. However, these require delicate balancing of forces and are likely unstable. Rotational effects remain largely unexplored except for the onset of the Gregory-Laflamme instability for equal spin black holes [13]. Beyond global $\mathrm{AdS}_5 \times \mathrm{S}^5$, there is freedom to choose a different gauge theory background than one conformal to $\mathbb{R}^{(t)} \times \mathrm{S}^3$. This can yield novel physics like plasma balls and boundary black holes (see [40] for a review), but none of these studies have included the effects of localisation.

Acknowledgements

O.D. acknowledges financial support from the STFC Ernest Rutherford grants ST/K005391/1 and ST/M004147/1. B.W. is supported by European Research Council grant no. ERC-2011-StG 279363-HiDGR. The authors thankfully acknowledge the computer resources, technical expertise and assistance provided by CENTRA/IST. Computations were performed at the cluster "Baltasar-Sete-Sóis" and supported by the H2020 ERC Consolidator Grant "Matter and strong field gravity: New frontiers in Einstein's theory" grant agreement no. MaGRaTh-646597.

* Electronic address: ojcd1r13@soton.ac.uk
† Electronic address: jss55@cam.ac.uk
‡ Electronic address: bw356@cam.ac.uk

[1] J. M. Maldacena, Int. J. Theor. Phys. **38**, 1113 (1999), [Adv. Theor. Math. Phys.2,231(1998)], hep-th/9711200.
[2] S. S. Gubser, I. R. Klebanov, and A. M. Polyakov, Phys. Lett. **B428**, 105 (1998), hep-th/9802109.
[3] E. Witten, Adv.Theor.Math.Phys. **2**, 253 (1998), hep-th/9802150.
[4] O. Aharony, S. S. Gubser, J. M. Maldacena, H. Ooguri, and Y. Oz, Phys. Rept. **323**, 183 (2000), hep-th/9905111.
[5] O. J. C. Dias, J. E. Santos, and B. Way, JHEP **04**, 060 (2015), 1501.06574.
[6] V. E. Hubeny and M. Rangamani, JHEP **0205**, 027 (2002), hep-th/0202189.
[7] R. Gregory and R. Laflamme, Phys.Rev.Lett. **70**, 2837 (1993), hep-th/9301052.
[8] T. Harmark and N. A. Obers, JHEP **0205**, 032 (2002), hep-th/0204047.
[9] B. Kol, JHEP **0510**, 049 (2005), hep-th/0206220.
[10] H. Kudoh and T. Wiseman, Phys.Rev.Lett. **94**, 161102 (2005), hep-th/0409111.
[11] T. Harmark, V. Niarchos, and N. A. Obers, Class.Quant.Grav. **24**, R1 (2007), hep-th/0701022.
[12] M. Headrick, S. Kitchen, and T. Wiseman, Class.Quant.Grav. **27**, 035002 (2010), 0905.1822.
[13] O. J. C. Dias, J. E. Santos, and B. Way (2015), 1510.02804.
[14] P. Figueras, J. Lucietti, and T. Wiseman, Class.Quant.Grav. **28**, 215018 (2011), 1104.4489.
[15] E. Witten, Adv.Theor.Math.Phys. **2**, 505 (1998), hep-th/9803131.
[16] K. Skenderis and M. Taylor, JHEP **0605**, 057 (2006), hep-th/0603016.
[17] H. Kim, L. Romans, and P. van Nieuwenhuizen, Phys.Rev. **D32**, 389 (1985).
[18] M. Gunaydin and N. Marcus, Class.Quant.Grav. **2**, L11 (1985).
[19] S. Lee, S. Minwalla, M. Rangamani, and N. Seiberg, Adv.Theor.Math.Phys. **2**, 697 (1998), hep-th/9806074.
[20] S. Lee, Nucl.Phys. **B563**, 349 (1999), hep-th/9907108.
[21] G. Arutyunov and S. Frolov, Phys.Rev. **D61**, 064009 (2000), hep-th/9907085.
[22] K. Skenderis and M. Taylor, JHEP **0608**, 001 (2006), hep-th/0604169.
[23] K. Skenderis and M. Taylor, JHEP **0709**, 019 (2007), 0706.0216.
[24] S. Hawking and D. N. Page, Commun.Math.Phys. **87**, 577 (1983).
[25] E. D'Hoker and D. Z. Freedman, in *Strings, Branes and Extra Dimensions: TASI 2001: Proceedings* (2002), pp. 3–158, hep-th/0201253.
[26] S. Catterall and T. Wiseman, JHEP **12**, 104 (2007), 0706.3518.
[27] K. N. Anagnostopoulos, M. Hanada, J. Nishimura, and S. Takeuchi, Phys. Rev. Lett. **100**, 021601 (2008), 0707.4454.
[28] S. Catterall and T. Wiseman, Phys. Rev. **D78**, 041502 (2008), 0803.4273.
[29] M. Hanada, Y. Hyakutake, J. Nishimura, and S. Takeuchi, Phys. Rev. Lett. **102**, 191602 (2009), 0811.3102.
[30] S. Catterall and T. Wiseman, JHEP **04**, 077 (2010), 0909.4947.
[31] M. Hanada, J. Nishimura, Y. Sekino, and T. Yoneya, JHEP **12**, 020 (2011), 1108.5153.
[32] M. Hanada, Y. Hyakutake, G. Ishiki, and J. Nishimura, Science **344**, 882 (2014), ISSN 0036-8075, http://science.sciencemag.org/content/344/6186/882.full.pdf, URL `http://science.sciencemag.org/content/344/6186/882`.
[33] B. A. Berg and T. Neuhaus, Phys. Rev. Lett. **68**, 9 (1992), URL `http://link.aps.org/doi/10.1103/PhysRevLett.68.9`.
[34] J. Lee, Phys. Rev. Lett. **71**, 211 (1993), URL `http://link.aps.org/doi/10.1103/PhysRevLett.71.211`.
[35] F. Wang and D. P. Landau, Phys. Rev. E **64**, 056101 (2001), URL `http://link.aps.org/doi/10.1103/PhysRevE.64.056101`.
[36] O. J. Dias, J. E. Santos, and B. Way, JHEP **1407**, 045 (2014), 1402.6345.
[37] R. Emparan, P. Figueras, and M. Martinez, JHEP **1412**, 072 (2014), 1410.4764.
[38] L. Lehner and F. Pretorius, Phys. Rev. Lett. **105**, 101102 (2010), 1006.5960.
[39] P. Figueras, M. Kunesch, and S. Tunyasuvunakool, Phys. Rev. Lett. **116**, 071102 (2016), 1512.04532.
[40] D. Marolf, M. Rangamani, and T. Wiseman, Class.Quant.Grav. **31**, 063001 (2014), 1312.0612.
[41] We only consider the strict $N \to +\infty$ limit.
[42] Our reference metric limits $\rho_0 < \pi$, but our solutions are well within this bound.

Supplementary Material

Ansatz

Here, we give our ansatz and reference metric in full. The ansatz in the $\{x, y\}$ coordinate system is given by

$$\mathrm{d}s^2 = \frac{L^2}{(1-y^2)^2}\left[-\frac{1}{L^2}H_1 f_1 \mathrm{d}t^2 + H_2\left(\frac{4f_2}{2-y^2}\mathrm{d}y^2 + y^2\left(2-y^2\right)f_3\,\mathrm{d}\Omega_3^2\right)\right]+ \\ + L^2 H_2\left[\frac{16}{2-x^2}f_4\left(\mathrm{d}x + f_6 \mathrm{d}y\right)^2 + 4x^2\left(2-x^2\right)\left(1-x^2\right)^2 f_5\,\mathrm{d}\Omega_4^2\right], \tag{1a}$$

$$C_{(4)} = L^3\frac{y^4\left(2-y^2\right)^2}{\sqrt{2}\left(1-y^2\right)^4}H_1 f_7\,\mathrm{d}t\wedge \mathrm{dS}_{(3)} + L^4 W\,\mathrm{dS}_{(4)}\,, \tag{1b}$$

where f_i are unknown functions, and the remaining quantities are known and given later below. The reference metric can be recovered by setting $f_i = 1$ for $i \neq 6$.

In the $\{\rho, \xi\}$ coordinate system, our ansatz is given by

$$\mathrm{d}s^2 = -M f_1\frac{\left(\rho^7-\rho_0^7\right)^2}{\left(\rho^7+\rho_0^7\right)^2}\mathrm{d}t^2 + L^2 H_2\left[\tilde{f}_2\mathrm{d}\rho^2 + \rho^2\left(\frac{4\tilde{f}_4(\mathrm{d}\xi + \tilde{f}_6\mathrm{d}\rho)^2}{2-\xi^2} + G_1\xi^2(2-\xi^2)f_3\mathrm{d}\Omega_3^2 + G_2\left(1-\xi^2\right)^2 f_5\,\mathrm{d}\Omega_4^2\right)\right], \tag{2a}$$

$$C_{(4)} = L^3\frac{\xi^4\left(2-\xi^2\right)^2\rho^4}{\sqrt{2}}M G_3 f_7\,\mathrm{d}t\wedge \mathrm{dS}_{(3)} + L^4 W\,d\mathrm{S}_{(4)}\,, \tag{2b}$$

where $\tilde{f}_2$, $\tilde{f}_4$, and $\tilde{f}_6$ are new unknown functions. The remaining functions transform as scalars. On the reference metric, these functions are $\tilde{f}_2 = 1$, $\tilde{f}_4 = 1$, and $\tilde{f}_6 = 0$.

There are a number of known functions where are given by

$$G_1 = \mathrm{sinc}\left(i\,\rho\,\xi\sqrt{2-\xi^2}\right)^2\,, \tag{3a}$$

$$G_2 = \mathrm{sinc}\Big(\rho\left(1-\xi^2\right)\Big)^2\,, \tag{3b}$$

$$H_1 = \frac{E_-^2}{E_+^2}\left(y^2\left(2-y^2\right)\frac{E_-^2}{E_+^2} + \left(1-y^2\right)^2\right)\,, \tag{3c}$$

$$H_2 = \left(1+\frac{\rho_0^7}{\rho^7}\right)^{4/7} = \left(1+\frac{\rho_0^7}{\left(\mathrm{arcsech}\left(1-y^2\right)^2 + 4\arcsin\left(1-x^2\right)^2\right)^{7/2}}\right)^{4/7}\,, \tag{3d}$$

$$M = 1 + \frac{\left(\rho_0^7-\rho^7\right)^2}{\left(\rho^7+\rho_0^7\right)^2}\sinh^2\left(\rho\,\xi\sqrt{2-\xi^2}\right)\,, \tag{3e}$$

where

$$E_\pm = \rho_0^7 \pm \left(4\arcsin\left(1-x^2\right)^2 + \mathrm{arcsech}\left(1-y^2\right)^2\right)^{7/2}\,. \tag{4}$$

and the function $\mathrm{sinc}z = \frac{\sin z}{z}$ for $z \neq 0$ and $\mathrm{sinc}z = 1$ for $z = 0$.

The relationship between $\{x, y\}$ and $\{\rho, \xi\}$ coordinate systems is given by

$$y = \sqrt{1-\mathrm{sech}\left(\rho\,\xi\sqrt{2-\xi^2}\right)}\,, \qquad x = \sqrt{1-\sin\left(\frac{1}{2}\rho\left(1-\xi^2\right)\right)}\,, \tag{5a}$$

$$\rho = \sqrt{\mathrm{arcsech}\left(1-y^2\right)^2 + 4\arcsin\left(1-x^2\right)^2}\,, \qquad \xi = \sqrt{1-\frac{2\arcsin\left(1-x^2\right)}{\sqrt{\mathrm{arcsech}\left(1-y^2\right)^2 + 4\arcsin\left(1-x^2\right)^2}}}\,. \tag{5b}$$

Holographic Stress Tensor and Kaluza-Klein holography

To find the energy E, the holographic stress tensor T_{ij} and the expectation value of holographic dual operators we need the asymptotic Taylor expansion of the fields around $y=1$ up to order $\mathcal{O}\left(1-y\right)^4$. This is given by

$$
\begin{aligned}
f_1\big|_{y=1} &= 1+\sqrt{\frac{5}{6}}\beta_2(1-y)^2Y_2(x)-\frac{1}{6}\sqrt{\frac{5}{2}}(1-y)^3\left(3\gamma_3Y_3(x)+2\sqrt{3}\beta_2Y_2(x)\right)\\
&+\frac{1}{192}(1-y)^4\Big[Y_0(x)\left(\left(40\beta_2^2+5\beta_2+12(16\delta_0+\delta_4-192)\right)-2304\right)\\
&+4\left(2\sqrt{30}\beta_2(8\beta_2+17)Y_2(x)+\left(18\sqrt{10}\gamma_3Y_3(x)+5\sqrt{7}\left(8\beta_2^2+\beta_2-4\delta_4\right)Y_4(x)\right)\right)\Big]+\mathcal{O}\left(1-y\right)^5, \qquad (6a)\\
f_2\big|_{y=1} &= 1+\sqrt{\frac{5}{6}}\beta_2(1-y)^2Y_2(x)-\frac{1}{6}\sqrt{\frac{5}{2}}(1-y)^3\left(3\gamma_3Y_3(x)+2\sqrt{3}\beta_2Y_2(x)\right)\\
&+\frac{(1-y)^4}{96}\Big[85\beta_2^2Y_0(x)+4\sqrt{30}(8\beta_2+17)\beta_2Y_2(x)\\
&+2\left(18\sqrt{10}\gamma_3Y_3(x)+5\sqrt{7}\left(8\beta_2^2+\beta_2-4\delta_4\right)Y_4(x)\right)\Big]+\mathcal{O}\left(1-y\right)^5, \qquad (6b)\\
f_3\big|_{y=1} &= 1+\sqrt{\frac{5}{6}}\beta_2(1-y)^2Y_2(x)-\frac{1}{6}\sqrt{\frac{5}{2}}(1-y)^3\left(3\gamma_3Y_3(x)+2\sqrt{3}\beta_2Y_2(x)\right)\\
&+\frac{1}{576}(1-y)^4\Big[Y_0(x)(2304-(5\beta_2+12(16\delta_0+\delta_4-192)))+\\
&12\left(2\sqrt{30}\beta_2(8\beta_2+17)Y_2(x)+\left(18\sqrt{10}\gamma_3Y_3(x)+5\sqrt{7}\left(8\beta_2^2+\beta_2-4\delta_4\right)Y_4(x)\right)\right)\Big]+\mathcal{O}\left(1-y\right)^5, \qquad (6c)\\
f_4\big|_{y=1} &= 1+\frac{1}{2}\sqrt{\frac{5}{6}}\beta_2(1-y)^2\left(45Y^x_{x\,(2)}(x)-\sqrt{30}Y_0(x)\right)\\
&-\frac{1}{240}(1-y)^3\Big[900\sqrt{30}\beta_2Y^x_{x\,(2)}(x)+525\sqrt{10}\gamma_3Y^x_{x\,(3)}(x)-600\beta_2Y_0(x)+512\sqrt{5}\gamma_1Y_1(x)-300\gamma_3Y_1(x)\Big]\\
&+(1-y)^4\Big[\frac{25}{1728\sqrt{7}}\left(8\beta_2^2+\beta_2-4\delta_4\right)\left(30\sqrt{210}Y^x_{x\,(2)}(x)+280Y^x_{x\,(4)}(x)-21\sqrt{7}Y_0(x)\right)\\
&+\frac{5}{6}\beta_2^2\left(4\sqrt{\frac{6}{5}}Y^x_{x\,(2)}(x)-\frac{4}{3}\sqrt{7}Y^x_{x\,(4)}(x)-\frac{7Y_0(x)}{16}\right)-\frac{17}{8}\sqrt{\frac{5}{6}}\beta_2\left(\sqrt{30}Y_0(x)-45Y^x_{x\,(2)}(x)\right)\\
&+\frac{15}{32}\gamma_3\left(7\sqrt{10}Y^x_{x\,(3)}(x)-4Y_1(x)\right)+\frac{16\gamma_1Y_1(x)}{\sqrt{5}}\Big]+\mathcal{O}\left(1-y\right)^5, \qquad (6d)\\
f_5\big|_{y=1} &= 1-\frac{1}{2}\sqrt{\frac{5}{6}}\beta_2(1-y)^2\left(180Y^\Omega_{\Omega\,(2)}(x)+\sqrt{30}Y_0(x)\right)\\
&+\frac{1}{60}(1-y)^3\Big[75\sqrt{10}\left(12\sqrt{3}\beta_2Y^\Omega_{\Omega\,(2)}(x)+7\gamma_3Y^\Omega_{\Omega\,(3)}(x)\right)+150\beta_2Y_0(x)+\left(75\gamma_3-128\sqrt{5}\gamma_1\right)Y_1(x)\Big]\\
&-\frac{(1-y)^4}{8640}\Big[75\left(7\left(46\beta_2^2+5\beta_2-20\delta_4\right)+1224\beta_2\right)Y_0(x)-216\left(128\sqrt{5}\gamma_1-75\gamma_3\right)Y_1(x)\\
&+120\sqrt{30}\left(1048\beta_2^2+5(918+25)\beta_2-500\delta_4\right)Y^\Omega_{\Omega\,(2)}(x)\\
&+200\left(567\sqrt{10}\gamma_3Y^\Omega_{\Omega\,(3)}(x)+4\sqrt{7}\left(8\beta_2^2+25\beta_2-100\delta_4\right)Y^\Omega_{\Omega\,(4)}(x)\right)\Big]+\mathcal{O}\left(1-y\right)^5, \qquad (6e)\\
f_6\big|_{y=1} &= \frac{1}{8}\sqrt{\frac{5}{2}}\beta_2\left(2-x^2\right)(1-y)S^{(2)}_x(x)+\left(2-x^2\right)(1-y)^2\Big[\gamma_1S^{(1)}_x(x)-\frac{1}{128}\sqrt{10}\left(12\beta_2S^{(2)}_x(x)+\sqrt{21}\gamma_3S^{(3)}_x(x)\right)\Big]\\
&-\left(2-x^2\right)(1-y)^3\Big[2\gamma_1S^{(1)}_x(x)-\frac{1}{48}\sqrt{\frac{5}{2}}\beta_2(8\beta_2+51)S^{(2)}_x(x)
\end{aligned}
$$

$$-\frac{1}{288}\sqrt{\frac{7}{2}}\left(9\sqrt{15}\gamma_3 S_x^{(3)}(x)+5\left(14\beta_2^2+\beta_2-4\delta_4\right)S_x^{(4)}(x)\right)\Bigg]+\mathcal{O}\left(1-y\right)^4\,, \tag{6f}$$

$$\begin{aligned} f_7\big|_{y=1} \;=\; & 1+\sqrt{\frac{10}{3}}\beta_2(1-y)^2Y_2(x)-\frac{1}{3}\sqrt{\frac{5}{2}}(1-y)^3\left(3\gamma_3Y_3(x)+2\sqrt{3}\beta_2Y_2(x)\right)\\ & +\frac{1}{360}(1-y)^4\Bigg[360\tilde{\delta}_0Y_0(x)+2\sqrt{30}\beta_2(128\beta_2+495)Y_2(x)\\ & +15\left(18\sqrt{10}\gamma_3Y_3(x)+\sqrt{7}\left(46\beta_2^2+5\beta_2-20\delta_4\right)Y_4(x)\right)\Bigg]+\mathcal{O}\left(1-y\right)^5\,, \end{aligned} \tag{6g}$$

where $Y_\ell(x)$, with $\ell=0,1,2,\cdots$ are the (regular) scalar harmonics of S^5 given by

$$Y_\ell(x)=\frac{\sqrt{3\pi}2^{\frac{1}{2}(-\ell-5)}\sqrt{(\ell+2)(\ell+3)}}{x^{3/2}\left(1-x^2\right)^{3/2}\left(2-x^2\right)^{3/4}}P_{\ell+\frac{3}{2}}^{-\frac{3}{2}}\left(-2x^4+4x^2-1\right), \tag{7}$$

$S_x^{(\ell)}(x)$ is the first component of the scalar derived vector harmonic $S_a^{(\ell)}$, and $Y^x_{x\,(\ell)}(x)$ and $Y^\Omega_{\Omega\,(\ell)}(x)$ are components of the scalar derived tensor harmonic $Y^a_{b\,(\ell)}(x)$ defined as

$$S_a^{(\ell)}=-\frac{1}{\sqrt{\ell(\ell+4)}}D_aY_\ell,\qquad\qquad Y^a_{b\,(\ell)}(x)=\frac{1}{\ell(\ell+4)}\,D^aD_bY_\ell+\frac{1}{5}\,\gamma^a{}_bY_\ell, \tag{8}$$

with γ_{ab} being the metric of the S^5.

In the above expansion we have already imposed the boundary conditions. The harmonic coefficients depend on six undetermined constants $\{\beta_2,\gamma_1,\gamma_3,\delta_0,\tilde{\delta}_0,\delta_4\}$. Two of these are gauge modes: γ_1 can be eliminated using diffeomorphisms while $\tilde{\delta}_0$ can be removed by a gauge transformation of $C_{(4)}$. Accordingly, no physical observable depends on $\gamma_1,\tilde{\delta}_0$. On the other hand, $\{\beta_2,\gamma_3,\delta_0,\delta_4\}$ are determined only after solving the entire boundary value problem. They vanish for $\mathrm{AdSSchw}_5\times\mathrm{S}^5$ and other solutions that preserve the full symmetries of the S^5, but not for solutions that break these symmetries. The reader interested on more details about these constants and their relation with the conformal dimensions of the holographic dual operators of the system is invited to read the detailed discussion in Appendix A.5 of [1].

With the above asymptotic expansion of the fields at the holographic boundary, we can compute the holographic stress tensor, the associated energy and expectation values of dual operators, which depend on the constants $\{\beta_2,\gamma_3,\delta_0,\delta_4\}$. We can do so using the formalism of Kaluza-Klein holography and holographic renormalisation [1, 2] (see also [3–9]). In particular, a detailed discussion of the formalism and expectation value computations for a system like ours that breaks the $SO(6)$ symmetry group of S^5 down to $SO(5)$ can be found in Appendix A of [1].

The expectation value of holographic stress tensor of our solutions is

$$\langle T_{ij}\rangle=\frac{N^2}{2\pi^2}\left[\frac{3}{16}+\frac{3}{4}-\frac{1}{3072}\left(30\beta_2^2+5\beta_2+12(16\delta_0+\delta_4-192)\right)\right]\,\mathrm{diag}\left\{1,\frac{1}{3}\,\eta_{\hat{i}\hat{j}}\right\}, \tag{9}$$

with $\eta_{\hat{i}\hat{j}}$ being the metric components of a unit radius S^3. This holographic stress tensor is conserved, $\nabla_i\langle T^{ij}\rangle=0$, and traceless, $\langle T_i{}^i\rangle=0$.

As usual in holographic renormalization, we can now use (9) to read the energy of the solution of our black holes (measured with respect to the global $\mathrm{AdS}_5\times\mathrm{S}^5$ solution):

$$E=\frac{N^2}{3072}\left[4608-\left(5\,\beta_2+30\,\beta_2^2+12\left(16\,\delta_0+\delta_4\right)\right)\right], \tag{10}$$

which, using (6a), can be rewritten as

$$\frac{EL}{N^2}=\frac{1}{512}\left(\partial_y^{(4)}f_3-\partial_y^{(4)}f_1\right)\big|_{y=1}\,. \tag{11}$$

Note that we have a static solution with a boundary metric that contains a symmetric S^3. By symmetry and the tracelessness of the stress tensor, all components of the stress tensor can be written in terms of the energy.

Kaluza-Klein holography also allows us to compute the expectation values of the scalar operators that condensate on the boundary theory when the $SO(6)$ R-symmetry of the scalar sector of $\mathcal{N}=4$ SYM is spontaneously broken. There is an infinite tower of such operators but one of them has the lowest conformal dimension, $\Delta = 2$. The expectation value of this operator $\mathcal{O}_2$ is

$$\langle \mathcal{O}_2 \rangle = -\frac{N^2}{\pi^2}\frac{1}{8}\sqrt{\frac{5}{3}}\,\beta_2, \tag{12}$$

and this is the expectation value that we that we show in Fig. 4 of the main Letter.

We can relate this expectation value to quantities in $\mathcal{N}=4$ SYM. Recall that the bosonic sector of $\mathcal{N}=4$ SYM contains six scalars X^i, here in the 6-dimensional rank-2 antisymmetric tensor representation of $SU(4)$ (recall that the groups $SU(4)$ and $SO(6)$ have isomorphic Lie algebras). There is also a spin-1 gauge field A_μ. The Lagrangian of this sector of the theory is given by [10]

$$\mathcal{L}^{(\text{bosonic})}_{\text{SYM}} = \text{Tr}\left(-\frac{1}{2\,g_{\text{YM}}^2}F_{\mu\nu}F^{\mu\nu} - \sum_i D_\mu X^i D^\mu X^i + \frac{1}{2}\,g_{\text{YM}}^2\sum_{i,j}\left[X^i, X^j\right]^2\right), \tag{13}$$

where $D_\mu X = \partial_\mu X + \mathrm{i}\,[A_\mu, X]$ is the gauge covariant derivative of the theory, $F_{\mu\nu} = \partial_\mu A_\nu - \partial_\nu A_\mu$ and g_{YM} is the dimensionless Yang-Mills gauge coupling. In terms of these fields, the expectation value in (12) can be written as [11]

$$\mathcal{O}_2 = \frac{2}{g_{\text{YM}}^2}\sqrt{\frac{5}{3}}\text{Tr}\left[(X^1)^2 - \frac{1}{5}\sum_{i=2}^{6}(X^i)^2\right], \tag{14}$$

though (14) uses the vector representation of $SO(6)$.

There is a technical detail that we have not mentioned. In the ansatz (1) and (2), there is a cross term which can in the $\{x, y\}$ coordinates be generally written schematically as $\sim (1-y^2)^p f_6 \mathrm{d}x\mathrm{d}y$, for some power p. Note that on the reference metric, we have $f_6 = 0$, so the reference metric is unaffected by p. However, our boundary condition $f_6 = 0$ at infinity ($y = 1$) *is* affected by the power p, since it determines the particular fall-off of the cross term. The choice of p therefore holds physical significance, and our choice of $p = 0$ is such that the various operators in the dual field theory are unsourced. For more details into how this power is determined, we refer the reader to the Appendix A.5 of [1].

For completeness, let us also give the explicit expressions for the temperature and the entropy. These are

$$TL = \frac{7}{2^{16/7}\pi}\frac{1}{\rho_0}\,, \tag{15a}$$

$$\frac{S}{N^2} = \frac{2^{44/7}\rho_0^8}{3}\int_0^1 d\xi\,\xi^3(2-\xi^2)(1-\xi^2)^4 f_3^{3/2}\tilde{f}_4^{1/2}f_5^2 G_1^{3/2}G_2^2\bigg|_{\rho=\rho_0}\,. \tag{15b}$$

Phase Diagram in the Canonical Ensemble

Below we give a phase diagram of our solutions in the canonical ensemble. In this ensemble, the temperature is fixed and the solution with the lowest free energy dominants. Fig. 1 shows the free energy FL/N^2 versus the temperature TL. In this ensemble, there is a first-order phase transition at the Hawking-Page point $\{FL/N2, TL\} = \{0, 3/(2\pi)\}$ between large black holes at higher temperatures and thermal AdS at lower. All other known solutions are subdominant to these.

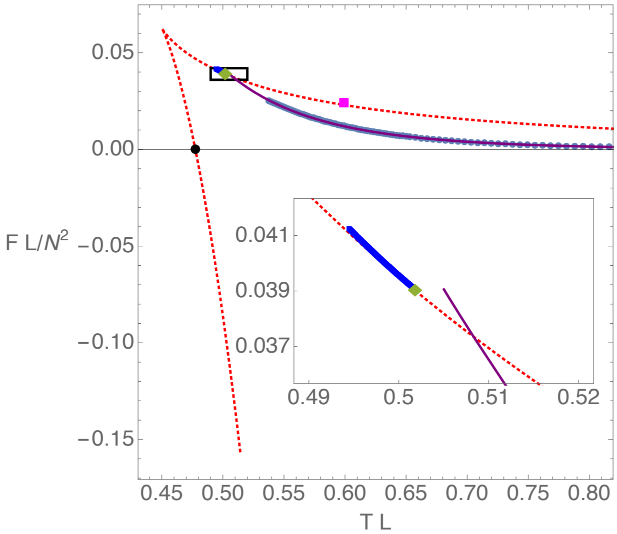

FIG. 1: Free energy vs Temperature. Same colour scheme as Fig. 3 of the main Letter. The black dot marks the Hawking-Page point, and the thin line with $F = 0$ represents thermal AdS.

Numerical validation and convergence

In this section, we perform a number of numerical checks. Let us first present convergence tests. Within each patch, we have use a $\widetilde{N} \times \widetilde{N}$ size grid. The convergence of a quantity Q can be shown through the function

$$R_Q(\widetilde{N}) = \left| 1 - \frac{Q_{\widetilde{N}}}{Q_{\widetilde{N}+1}} \right| , \tag{16}$$

which vanishes for large $\widetilde{N}$ for any converging numerical method. Since we are using pseudospectral collocation, R_Q should decrease exponentially in $\widetilde{N}$ if the solution is sufficiently smooth. Since our reference metric has been adapted for small black holes, it is especially difficult to perform accurate numerics on large black holes. We therefore perform convergence tests for localised black holes with $\rho_0 = 0.85$ which is the largest value we have reached. In Fig. 2 we present convergence tests for the quantities $Q = \langle \mathcal{O}_2 \rangle$ and $Q = E$, both of which show exponential convergence.

We can also test our numerics by using proven identities for solutions. For instance, the energy extracted at infinity via Kaluza-Klein holography needs to be equal to the energy extracted by integrating the first law. We find that these agree numerically to within 0.1% error.

The first law, however, does not test all components of the Einstein equation. A more stringent test can be made by investigating Komar identities, similar to the ones presented in [12]. For every Killing vector ξ^M of our solution we can define an antisymmetric conserved tensor

$$(K_\xi)^{MN} = \nabla^M \xi^N - \frac{1}{12} F_{(5)}^{MNPQR} \xi^U C_{(4)\,PQRU} + \gamma \xi^{[M} F_{(5)}^{N]PQRU} C_{(4)\,PQRU} \,, \tag{17}$$

where $F_{(5)} = \mathrm{d}C_{(4)}$ and γ is an arbitrary constant. Conservation of this tensor follows from the Einstein equation, $\nabla^M F_{(5)\,MNPQR} = 0$, and from the identities

$$\mathcal{L}_\xi g = \mathcal{L}_\xi C_4 = \mathcal{L}_\xi F_5 = 0 \,, \quad \nabla_M \nabla^M \xi_N = -R_{NM} \xi^M \quad \text{and} \quad F_{(5)} = \star F_{(5)} \,, \tag{18}$$

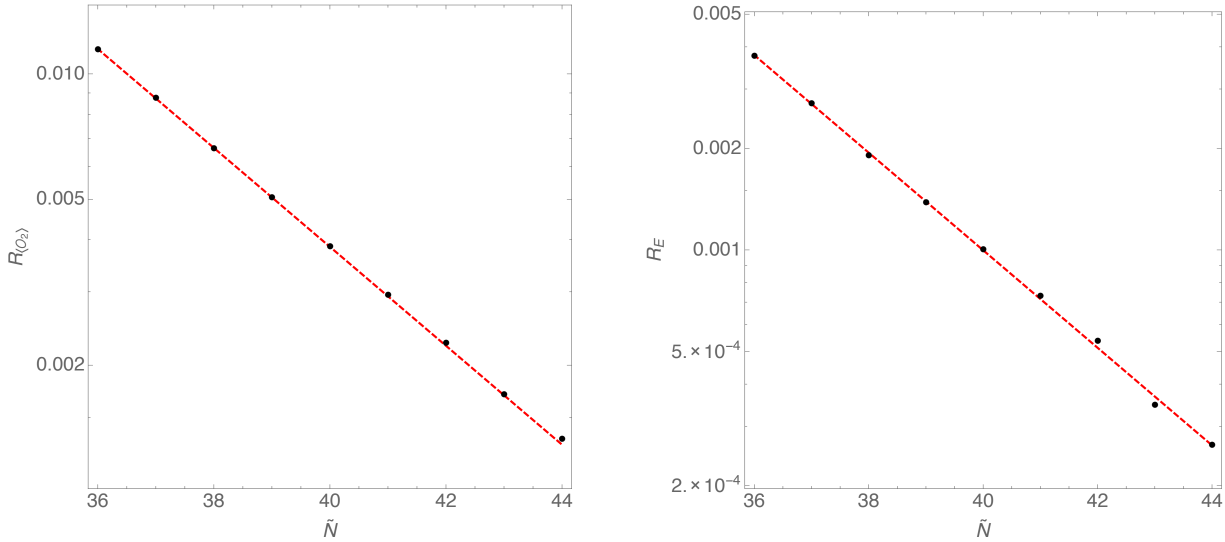

FIG. 2: Convergence of $\langle\mathcal{O}_2\rangle$ (on the left) and E (on the right) and as a function of $\widetilde{N}$ for $\rho_0 = 17/20$.

where $\mathcal{L}_\xi$ is the Lie derivative along ξ.

In the language of differential forms, this means that we have a closed 8-form

$$\mathrm{d}(\star K_\xi) = 0\,, \tag{19}$$

where

$$K_\xi = \frac{1}{2}(K_\xi)_{MN}\mathrm{d}x^M \wedge \mathrm{d}x^N\,. \tag{20}$$

Integrating $\mathrm{d}(\star K_\xi)$ over a 9−dimensional surface Σ of constant time with $y_1 < y < y_2$, we conclude that

$$0 = \int_\Sigma \mathrm{d}(\star K_\xi) = \int_{\partial\Sigma} \star K_\xi = \int_{\Gamma(y_1)} \star K_\xi - \int_{\Gamma(y_2)} \star K_\xi + \int_{\text{Dirac}} \star K_\xi\,, \tag{21}$$

where we used the fact that the boundary of Σ has two disjoint components $\Gamma(y_1)$ and $\Gamma(y_2)$ (with opposite orientations). The last term come from the contribution of a Dirac string, which we will now explain. At infinity, $F_{(5)} = \mathrm{d}C_{(4)}$ contains a term proportional to the S^5 volume form $\mathrm{d}S_{(5)}$, which implies that $C_{(4)}$ cannot be made everywhere regular on the S^5. One can choose $C_{(4)}$ to be regular at the north pole of the S^5, say, but not at the south pole of the S^5. In other words, $C_{(4)}$ has a Dirac string, which we must integrate over. However, we find that for $\gamma = 0$, the last term is actually absent. From here onwards, we take γ to be zero.

This shows that (for $\gamma = 0$) the integral

$$I_\xi(y) = \int_{\Gamma(y)} \star K_\xi \tag{22}$$

over the closed surface of constant time and radial coordinate y is independent of the value of y. The Komar formula is obtained by equating the integral over the horizon $I_\xi(0)$, which can be written in terms of the entropy and the temperature, to the integral at infinity $I_\xi(1)$, which can be written in terms of the asymptotic quantities of the previous section.

$$\frac{ST}{N^2} = \frac{36\,(192 - 8\delta_0 - \delta_4) - \beta_2\,(86\beta_2 + 207)}{4608}\,. \tag{23}$$

Note that in our setup, this identity relates quantities on different patches and different coordinate systems. We have tested this identity, and we find agreement up to 0.1%.

Since our numerics were unable to reach the phase transition between localised black holes and $\mathrm{AdSSchw}_5 \times \mathrm{S}^5$ black holes, we had to use extrapolation to obtain the location of the phase transition. We preform this extrapolation by a motivated χ^2 fit to our data on the $\Delta S(EL/N^2)/N^2$ curve (recall ΔS is the entropy with respect to that of $\mathrm{AdSSchw}_5 \times \mathrm{S}^5$). Our fitting function was chosen to be

$$\Delta S_{\mathrm{fit}}(x)/N^2 = \frac{105^{1/7}\pi^{8/7}x^{8/7}}{2^{12/7}}\left(1 + a_0 x^{\alpha} + b_0 x^{\alpha+1}\right) . \tag{24}$$

The first term in the fitting function was chosen so that it matches the entropy of a ten-dimensional asymptotically flat Schwarzschild black hole at small energies (small x). There are a total of three fitting parameters: a_0, b_0 and α. A χ^2 fit yields the values and associated errors $\alpha = 0.190576(1 \pm 0.0019)$, $a_0 = -0.12688(1 \pm 0.0011)$ and $b_0 = 0.187541(1 \pm 0.0026)$. We can then find the transition point from a simple root-finding algorithm. This occurs for $EL/N^2 \approx 0.225(1 \pm 0.0027)$, which is the value we quote in the main text. The error obtained for the crossing can be computed by propagating the error associated with each of the parameters in the fit.

To test the sensitivity of this result to other extrapolation methods, we have also performed an order-p polynomial interpolation on the last $p+1$ data points for p from 3 to 10, then extrapolating this polynomial to the phase transition. The largest deviation from $EL/N^2 \approx 0.225$ was under 2%.

[1] O. J. C. Dias, J. E. Santos, and B. Way, JHEP **04**, 060 (2015), 1501.06574.
[2] K. Skenderis and M. Taylor, JHEP **0605**, 057 (2006), hep-th/0603016.
[3] H. Kim, L. Romans, and P. van Nieuwenhuizen, Phys.Rev. **D32**, 389 (1985).
[4] M. Gunaydin and N. Marcus, Class.Quant.Grav. **2**, L11 (1985).
[5] S. Lee, S. Minwalla, M. Rangamani, and N. Seiberg, Adv.Theor.Math.Phys. **2**, 697 (1998), hep-th/9806074.
[6] S. Lee, Nucl.Phys. **B563**, 349 (1999), hep-th/9907108.
[7] G. Arutyunov and S. Frolov, Phys.Rev. **D61**, 064009 (2000), hep-th/9907085.
[8] K. Skenderis and M. Taylor, JHEP **0608**, 001 (2006), hep-th/0604169.
[9] K. Skenderis and M. Taylor, JHEP **0709**, 019 (2007), 0706.0216.
[10] E. D'Hoker and D. Z. Freedman, in *Strings, Branes and Extra Dimensions: TASI 2001: Proceedings* (2002), pp. 3–158, hep-th/0201253.
[11] E. Witten, Adv.Theor.Math.Phys. **2**, 253 (1998), hep-th/9802150.
[12] M. S. Costa, L. Greenspan, J. Penedones, and J. Santos, JHEP **03**, 069 (2015), 1411.5541.